time delays involved for possible laser oscillation on 8-7, 7-6, ···, 2-1 bands. The population inversion travels down the vibrational level ladder in the form of a wave, i.e., first the 10-9 band is inverted, then the 9-8, 8-7 and so on.

This trend, however, is in a direction opposite to the experimentally determined delays. We see from Table I that the 6-5 band starts oscillating first, then the 7-6 and so on, and 10-9 oscillates last, i.e., the disturbance caused by laser oscillation travels upward to cause inversion. Also we see that the analysis with these assumptions predicts that inversion should also be established between the 5-4, 4-3, ···, 2-1 levels at longer times, which is not found to be the case in experimental investigations. No laser action was detected for vibrational levels $v<5$. In light of the three simple cases analyzed and the experimental findings, we have to conclude that the excitation conditions are not as simple as those described in (2) and (3) even under pulsed operation. The levels $v<5$ are populated very heavily so that no laser oscillation takes place on P branch rotational transitions for these bands with $v<5$. In the above two pulsed operation examples, it was seen the J for maximum gain on a P-branch rotational transition shifts with time. This is not borne out by experimental findings. This implies that presumably with a given vibrational band, different rotational transitions oscillate at different times. But, experimentally, it was seen that *all* the rotational transitions belonging to one vibrational band started oscillating approximately at the same time. This also implies complicated and time-dependent excitation processes n_v which may involve recombination in addition to cascading from higher electronic levels.

ACKNOWLEDGMENTS

The author thanks R. J. Kerl for excellent technical assistance and Mrs. C. A. Lambert for aid in computer calculations.

PHYSICAL REVIEW VOLUME 141, NUMBER 1 JANUARY 1966

Excitation-Transfer Collisions between Rubidium and Helium Atoms

T. J. BEAHN, W. J. CONDELL, AND H. I. MANDELBERG
Laboratory for Physical Sciences, 7338 Baltimore Avenue, College Park, Maryland
(Received 10 June 1965; revised manuscript received 2 September 1965)

An experiment is described which measures the collision cross section for transfer of excitation in rubidium by helium. Rubidium atoms are pumped to either the $^2P_{1/2}$ or $^2P_{3/2}$ state by irradiation with one of the resonance lines. Some excited rubidium atoms are transferred to the other P state by collisions with helium atoms. The rubidium atoms then radiate both resonance lines. Measurements of the intensities of both resonance lines as a function of helium pressure are used to calculate the collision cross section. The cross section for $^2P_{1/2}$ to $^2P_{3/2}$ is 1.0×10^{-17} cm$^2\pm10\%$ and for $^2P_{3/2}$ to $^2P_{1/2}$ is 1.2×10^{-17} cm$^2\pm10\%$.

I. INTRODUCTION

THE effect of rare-gas collisions with sodium atoms excited to the $^2P_{1/2}$ or $^2P_{3/2}$ states was first observed by Wood.[1] Subsequently, Lochte-Holtgreven[2] repeated Wood's experiments, and from his data cross sections for the transfer between the two states by rare gases can be found. More recently, similar work has been done by Seiwert,[3] Jordan,[4] and by Krause and his co-workers.[5,6] Recent interest in optical pumping of rubidium in rare-gas buffered cells as well as interest in the fundamental processes involved prompted us to examine the interaction of excited rubidium atoms with helium.

Rubidium is particularly well suited for such investigation because it has sufficient vapor pressure at easily attained temperatures and the resonance lines, lying at 7800 and 7947 Å, are easily isolated with interference filters.

If rubidium vapor is irradiated with D_1 radiation (7947 Å) from a rubidium light source, it will in the presence of helium gas reradiate not only D_1 light but also D_2 (7800 Å). The relative amount of D_2 will depend on the amount of helium gas present. By varying the amount of helium gas, we can find a collision cross section for the transfer from $^2P_{1/2}$ to $^2P_{3/2}$. Similarly, if the rubidium vapor is irradiated with D_2 light, it will reradiate D_1 in addition to D_2 because of the collisions with helium. Again, by varying the amount of helium present we can find the cross section for the transfer $^2P_{3/2}$ to $^2P_{1/2}$. The transfer can also be caused by the excited rubidium atom colliding with a ground-state

[1] R. W. Wood, Phil. Mag. 27, 1018 (1914).
[2] W. Lochte-Holtgreven, Z. Physik 47, 362 (1928).
[3] R. Seiwert, Ann. Physik 18, 54 (1956).
[4] J. A. Jordan, Ph.D. thesis, University of Michigan, 1964 (unpublished).
[5] G. D. Chapman and L. Krause, Can. J. Phys. 43, 563 (1965).
[6] G. D. Chapman, M. Czajkowski, A. G. A. Rae, and L. Krause, Abstracts of the IVth International Conference on the Physics of Electronic and Atomic Collisions; Quebec, Canada, 1965, p. 55 (unpublished).

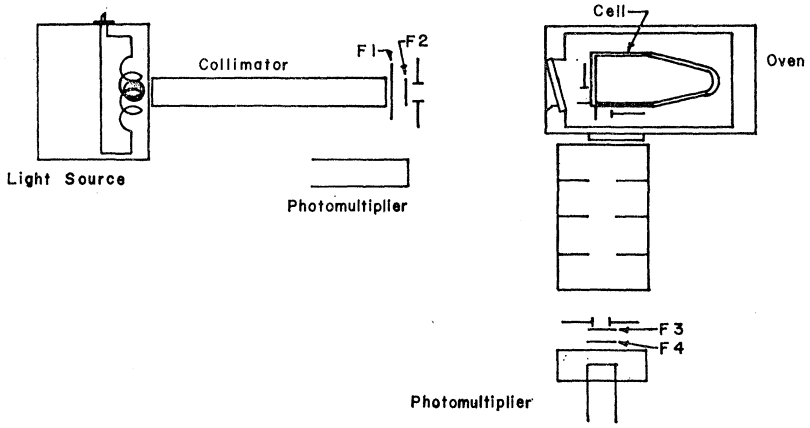

FIG. 1. This sketch shows the main features of the apparatus drawn roughly to scale. The filters are indicated in the input beam by $F1$ and $F2$ and on the output by $F3$ and $F4$. Photomultipliers were used for monitoring the light source intensity and for observation of the fluorescence. The horn containing the metal deposit is not shown.

rubidium atom. Quenching collisions, causing radiationless de-excitation can also take place.

The rate equations for the processes described can be easily written. Numbering the ground, $^2P_{1/2}$, and $^2P_{3/2}$ states of rubidium with subscripts 0, 1, and 2, respectively, we can write

$$dn_1/dt=S_1+n_2n_0\beta_{21}+n_2N_0\alpha_{21}-n_1A_{10} -n_1N_0Q_{10}-n_1N_0\alpha_{12}-n_1n_0\beta_{12}. \quad (1)$$

The n's are the population densities of the various rubidium states, the α's are the frequencies of excitation transfer collisions by helium, the β's are the frequencies of excitation transfer by rubidium collisions, the Q's are the frequencies of quenching collisions, and N_0 is the helium gas number density. Examining the terms in order, we find that the first, S_1, is due to the absorption of D_1 radiation from the light source, the only irradiation assumed present. The second and third terms come from transfer collisions with rubidium and helium, respectively. The depopulation processes are contained in the fourth through seventh terms and are due to spontaneous emission, quenching, helium transfer collisions, and rubidium transfer collisions, respectively. Neglected in this equation are three-body collisions. Experimental results justify the omission. The time rate of change of the population density of the $^2P_{3/2}$ state can be written:

$$dn_2/dt=n_1N_0\alpha_{12}+n_1n_0\beta_{12}-n_2A_{20} -n_2N_0Q_{20}-n_2N_0\alpha_{21}-n_2n_0\beta_{21}. \quad (2)$$

The first and second terms come from transfer collisions with helium and rubidium, respectively. The third comes from depopulation by spontaneous emission. The fourth comes from quenching while the last two from transfer collisions with helium and rubidium in order.

Equations (1) and (2) yield for the steady state the ratio of the excited-state densities

$$\frac{n_1}{n_2}=\frac{N_0(Q_{20}+\alpha_{21})+n_0\beta_{21}+A_{20}}{N_0\alpha_{12}+n_0\beta_{12}}. \quad (3)$$

The terms associated with rubidium transfer collisions, $n_0\beta_{12}$ and $n_0\beta_{21}$, were found experimentally to be negligible with respect to the helium transfer collisions. Therefore, Eq. (3) may be reduced to

$$\frac{n_1}{n_2}=\frac{A_{20}}{\alpha_{12}}\left(\frac{1}{N_0}\right)+\frac{Q_{20}+\alpha_{21}}{\alpha_{12}}. \quad (4)$$

When the rubidium vapor pressure in the resonance cell is low enough that there is no resonance radiation entrapment, the ratio of the population of states will be directly proportional to the ratio of the reradiated light intensities. The intensity ratio can then be written

$$\frac{I_1}{I_2}=\frac{K_1}{\alpha_{12}}\left(\frac{1}{P}\right)+K_2, \quad (5)$$

where I_1 and I_2 are the intensities of the emitted D_1 and D_2 lines, K_1 is a calculable constant, and P is the helium gas pressure. The collision cross section for excitation transfer caused by the helium is σ_{12} and is related to the excitation transfer frequency α_{12} by the average relative velocity

$$\sigma_{12}=\alpha_{12}/\bar{V}_R(T).$$

If, instead of using D_1 irradiation, we use D_2, similar rate equations can be written. Solution of them under the same conditions used to get Eq. (5) gives the following:

$$\frac{I_2}{I_1}=\frac{C_1}{\alpha_{21}}\left(\frac{1}{P}\right)+C_2, \quad (6)$$

the notation being the same as before.

From Eqs. (5) and (6) we see that the cross sections, σ_{12} and σ_{21}, appear as factors in the slope of the intensity ratio as a function of the reciprocal of the helium gas pressure. The other factor in the slope, K_1 or C_1, contains known constants. These constants are the appropriate spontaneous dipole transition probability, measurable instrumental characteristics, and physical constants. The experimental method thus consists of

measuring the intensity ratio as a function of the helium pressure, finding the slope, and then calculating the cross sections from the observed slope and the known constants. It should be noted that neither the rubidium number density nor the irradiating light intensity explicitly enters Eqs. (5) and (6). All that is required is that both either remain constant during the series of measurements or that the observed reradiated intensities be suitably normalized.

II. EXPERIMENTAL DETAILS

A sketch of the experimental apparatus is shown in Fig. 1. It consisted of an rf excited rubidium light source, a glass cell containing the rubidium vapor and a controllable amount of helium gas, and interference filters for selective irradiation and observation of the resonance lines. The glass cell was made from 2-in. sq Pyrex tubing with the standard horn termination. The horn, which constituted the rubidium reservoir was immersed in an oil bath which was stirred and could be maintained at a temperature constant to $\pm 0.1°C$ over several hours.

The cell was surrounded by an oven which kept the cell at about 100°C. This was necessary to prevent the rubidium vapor from depositing on the cell walls. Even though the cell was kept at 100°C, the rubidium vapor pressure was controlled by the horn temperature, somewhat below the oven temperature. At the lowest vapor pressures, it was necessary to cool the oil bath with water because some heat from the oven was transferred to the rubidium reservoir. In all cases the rubidium reservoir was maintained within $\pm 0.1°C$.

The entrance window of the oven was installed at an angle of 15 deg with the incident radiation so that a portion of the incident radiation was specularly reflected to a photomultiplier, the signal from which was used to normalize the measurements.

The light source was a spherical bulb of 3-cm diameter into which a small amount of rubidium was distilled. Krypton was added to a pressure of 30 mm Hg, and the bulb sealed off. The source was excited by a 50-Mc/sec rf supply, and showed good short-term stability in light output. Over one day the light output varied no more than 5%. The monitoring of its output and subsequent normalization of the data eliminated consideration of the light source as contributing to the experimental error. The light source was mounted 15 in. from the entrance window of the cell. A lensless collimator limited the angle of the extreme rays from the light source to 1.5 deg in the horizontal plane and 6 deg in the vertical. Two interference filters were placed in the input beam at distances of 9 and 10 in. from the light source.

A stop was placed in front of the cell's entrance window, and this stop limited the irradiated area to 1.5×2.0 cm. The reradiated light was observed at right angles to the incident beam through a stop of the same dimensions. The volume observed within the cell was thus about 4.5 cm^3.

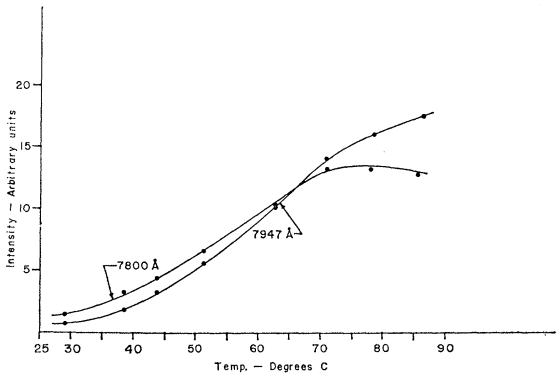

FIG. 2. The total intensity of the D_1 and D_2 lines in fluorescence as a function of rubidium reservoir temperature. The D_2 line is strongly absorbed and the intensity decreases above 75°C.

The reradiated light was measured with an RCA No. 7102 photomultiplier which was cooled by passing the efflux gas from boiling liquid nitrogen over its face. Between this photomultiplier and the cell were placed two interference filters. One was 5.5 in. from the cell, and the other 6 in. Both had circular apertures of $\frac{7}{8}$-in.-diameter, forming the limiting stop of the system.

The interference filters all had about 70% transmission at the peak band pass. The transmission of a typical band-pass filter for 7947 Å showed less than 0.2% transmission at 7800 Å while that of a 7800-Å filter showed less than 0.4% at 7947 Å. More exact measurements were made on each filter, and they showed that when the filters were used in pairs, no difficulty arose from leakage of the unwanted radiation. The transmission factors of the filters used in the reradiated beam entered directly into the constants in Eqs. (5) and (6). Therefore, the transmission factors were measured under the same conditions as the data were taken. This was done by measuring the transmission with one filter, then two and was done for each filter used. The transmission of the combination was taken to be the product of the transmissions of the two. Multiple reflections between the filters were neglected as the filter absorption was high and the solid angle used was large enough to average over any interference effects between the two filters.

The vacuum system had an ultimate vacuum in the 10^{-7}-Torr range. To insure good gas purity we used liquid-nitrogen cold-trapping and a uranium getter. Occassionally a dc discharge was run in the gas filling system so that a check on the gas purity could be made using cataphoretic accumulation. The helium pressures used ranged from about 20 to 400 mm Hg. The pressures below 100 mm were measured with an Octoil-S manometer while the higher pressures were measured with a mercury manometer having an Octoil-S film over the mercury.

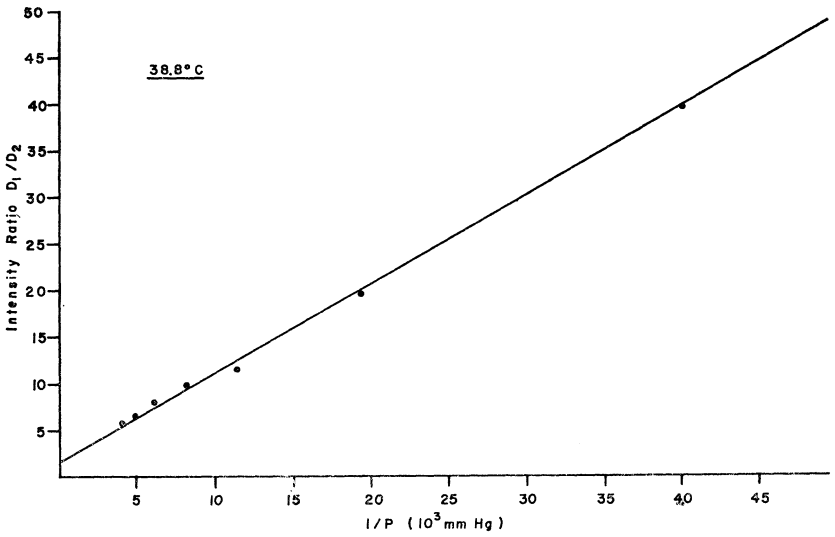

FIG. 3. The measured intensity ratio D_1/D_2 for D_1 illumination as a function of $1/P$ for 38.8°C rubidium reservoir temperature.

Preliminary checks were made on the degree of polarization in the reradiated light. It was found that with helium pressures above 20 or 25 mm Hg, no significant degree of polarization remained. Consequently, it was not necessary to use polarizers in either input or output beams.

III. RESULTS

It was necessary to determine the region of rubidium vapor pressure for which there would be negligible radiation entrapment yet enough reradiation for detection. Measurements were taken of the resonance fluorescence, both D_1 and D_2 separately, as a function of the rubidium reservoir temperature with no helium present. The results are shown in Fig. 2. It is seen that below 35 to 40°C negligible entrapment took place, and the cross sections reported are based on measurements below those temperatures.

Typical plots of the intensity ratios as a function of the reciprocal of the helium pressure in the cell, are given in Figs. 3 and 4. These are for a rubidium reservoir temperature of 38.8°C. Plots for all other temperatures show the same features. In Figs. 3 and 4 the data points range from about 20 to 300 mm Hg. From these data, as well as those taken at other rubidium vapor pressures, the slope of the plot was found with a least-squares method.

The slopes obtained at various rubidium temperatures are shown as a function of that temperature in Figs. 5 and 6. The data points range over a factor of 40 in rubidium vapor pressure in these plots. Effects

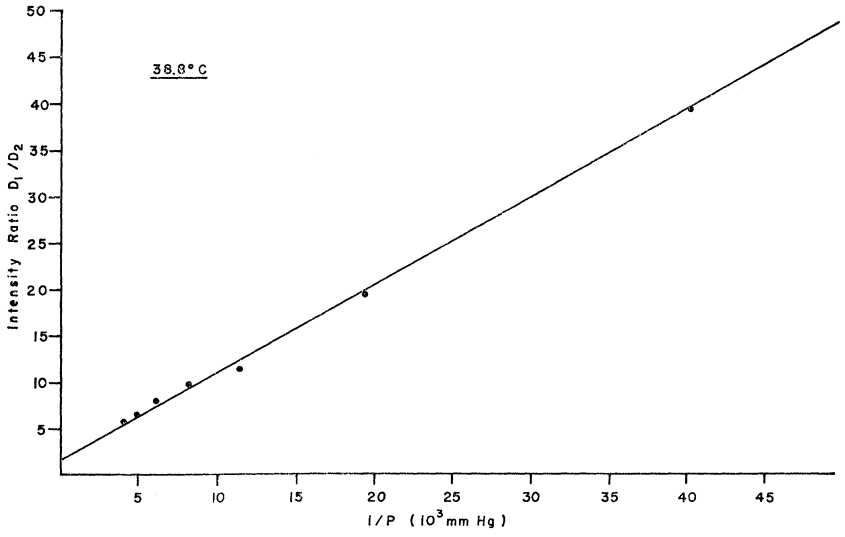

FIG. 4. The measured intensity ratio D_2/D_1 for D_2 illumination as a function of $1/P$ for 38.8°C rubidium reservoir temperature.

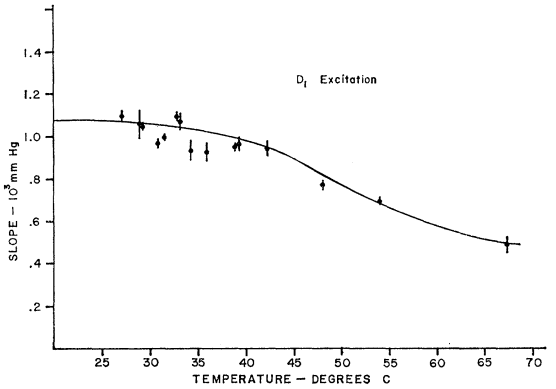

FIG. 5. The measured slopes for D_1 excitation as a function of Rb reservoir temperature.

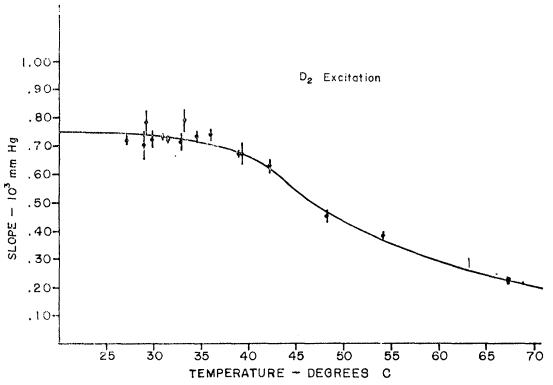

FIG. 6. The measured slopes for D_2 excitation as a function of Rb reservoir temperature.

unaccounted for in Eqs. (5) and (6) should disappear at very low rubidium vapor pressures. So a reasonable line was drawn through the data points of Figs. 5 and 6 and limiting values of the slopes were found. For D_2 excitation the limiting value was 0.75×10^3 (mm Hg) and for D_1, 1.08×10^3 (mm Hg). Whatever the cause for the change in slope at higher temperatures, be it radiation entrapment, three-body collisions, or what have you, these extrapolated slopes should truly be representative of the model used for the rate equations.

From these slopes the cross sections were computed. The dipole transition probabilities given by Heavens[7] were used. Since the cell was kept at 100°C, the cross sections are for that temperature. For the transfer of rubidium from $^2P_{1/2}$ to $^2P_{3/2}$ by helium the cross section, σ_{12}, is 1.0×10^{-17} cm$^2\pm10\%$. For the reverse, σ_{21}, it is 1.2×10^{-17} cm$^2\pm10\%$. The errors arise principally from the uncertainty in the slopes and the measurement of the filter transmissions.

From Eq. (4), we would have expected the intercepts such as those obtained from Figs. 3 and 4 to give the ratio of the cross sections if quenching can be neglected ($Q_{20}=0$). Unfortunately, the deviations of the intercepts of the fitted straight lines was so great that on this basis we could not even say which cross section was larger. However, a prediction of the ratio of the cross sections is possible. Using the relation of Klein and Rosseland[8] and assuming a Maxwellian distribution of velocities (or alternately, just applying detailed balance) the ratio of cross sections should be

$$\frac{\sigma_{12}}{\sigma_{21}}=\frac{g_2}{g_1}\exp\left[\frac{-\Delta E}{kT}\right], \tag{7}$$

where the g's are the degeneracies and ΔE is the energy difference between the $^2P_{3/2}$ and $^2P_{1/2}$ states (0.030 eV). At 373°K Eq. (7) predicts that σ_{12} should equal 0.78 σ_{21}. Within experimental error the measured cross sections agree with this relation.

Table I is a summary of the alkali–rare-gas cross sections for helium, neon, and argon which have been published to date. It includes our preliminary results on rubidium-neon and rubidium-argon collisions, obtained in the same way as the rubidium-helium cross sections. These cross sections are at least an order of magnitude smaller than the corresponding helium cross sections, an effect which is not evidenced in the other alkalis.

TABLE I. Cross sections $^2P_{3/2}$-$^2P_{1/2}$, $^2P_{1/2}$-$^2P_{3/2}$ for helium, neon, and argon mixing.[a]

Alkali	Rare gas	σ_{12} (Å^2)	σ_{21} (Å^2)	References
Na	He	77[b]	41.1	4
Na	Ne	68[b]	36.1	4
Na	Ar	121[b]	64.6	4
Na	Ar	100	60	3
K	He	84[b]	52.8	4
K	He	60	41	6
K	Ne	22[b]	14	4
K	Ne	11	7	6
K	Ar	54[b]	34	4
K	Ar	26	16	6
Rb	He	0.10	0.12	This work
Rb	Ne	10^{-3}–10^{-2}	10^{-3}–10^{-2}	This work
Rb	Ar	10^{-3}–10^{-2}	10^{-3}–10^{-2}	This work
Cs	He	4.0×10^{-5}	2.7×10^{-4}	6
Cs	Ne	1.9×10^{-5}	3.1×10^{-4}	6
Cs	Ar	1.6×10^{-5}	5.2×10^{-4}	6

[a] The temperature of the rare-gas–alkali vapor mixture varies somewhat among these measurements. See individual references for exact temperatures.
[b] Calculated from σ_{21} according to Eq. (7) but not directly measured.

[7] O. S. Heavens, J. Opt. Soc. Am. **51**, 10 (1961).

[8] O. Klein and S. Rosseland, Z. Physik **4**, 46 (1921).